Available online at www.sciencedirect.com
SCIENCE DIRECT
International Journal of Heat and Mass Transfer 49 (2006) 4279–4289
International Journal of HEAT and MASS TRANSFER
www.elsevier.com/locate/ijhmt

Modeling the effects of surface roughness on the emissivity of aluminum alloys

Chang-Da Wen, Issam Mudawar *

Boiling and Two-phase Flow Laboratory, School of Mechanical Engineering, Purdue University, West Lafayette, IN 47907, USA

Received 25 May 2005; received in revised form 7 April 2006

Abstract

This study explores the relationship between the emissivity of aluminum alloy surfaces and surface roughness. Two methods are discussed which yield good overall predictions of the emissivity of rough surfaces. One method consists of using a mathematical multispectral radiation thermometry (MRT) model for the emissivity and determining both the surface temperature and the empirical constants in the emissivity model from radiance measurements. This method requires new emissivity constants to be determined for each surface topography. This study also presents an alternative method for determining the emissivity of rough surfaces. This method relies on determining the emissivity characteristics of a single reference surface and inferring the emissivity of any other rough surface of the same material by relating a surface roughness function (determined by surface topography instrumentation) of the rough surface to that of the reference surface. Using data for AL 7075 with various degrees of surface roughness, this method is shown to yield better accuracy than the first method.

1. Multispectral radiation thermometry (MRT) methods

Most processes in aluminum production, such as extruding and rolling, are highly temperature-dependent. For example, achieving superior microstructure and mechanical properties during extrusion requires precise knowledge of the part's temperature during transit. Therefore, accurate temperature determination and control are of paramount importance in the quest for superior alloys, lower cost and reduced waste.

Sensors requiring physical contact with a surface such as thermocouples are widely used for temperature measurement in many industries. However, the fast transit of extruded parts often reduces the accuracy of contact sensors to no better than 10 K [1].

Radiation thermometry is a popular alternative to contact temperature measurement. This non-contact measurement method utilizes spectral radiance observation from the target surface to infer the surface temperature. The temperature is determined using one of three categories of radiation thermometry: spectral, dual-wavelength and multispectral. Spectral radiation thermometry requires radiance measurement at one wavelength and a constant emissivity value to infer the surface temperature. Dual-wavelength radiation thermometry (DWRT) utilizes radiance measurements at two wavelengths and an emissivity compensation algorithm. Multispectral radiation thermometry (MRT) employs radiance measurements at three or more wavelengths and an emissivity model. Due to their inability to adequately compensate for the complex emissivity characteristics of aluminum alloys, the spectral and dual-wavelength methods have been used only in well-defined and well-controlled situations [2]. The present study is focused entirely on MRT methods.

Two different mathematical techniques are used to infer temperature using MRT. The first is the *exact technique* which utilizes an emissivity model with n unknown coefficients, and radiation intensity measurements at $n+1$

* Corresponding author. Tel.: +1 765 494 5705; fax: +1 765 494 0539.
E-mail address: mudawar@ecn.purdue.edu (I. Mudawar).

0017-9310/$ - see front matter © 2006 Elsevier Ltd. All rights reserved.
doi:10.1016/j.ijheatmasstransfer.2006.04.037

Nomenclature

A	surface area
BDRF	bidirectional reflectance function
c_1	first thermal radiation constant
c_2	second thermal radiation constant
DWRT	dual-wavelength radiation thermometry
E_b	blackbody radiation
F	view factor
$L_{\lambda,\mathrm{gen}}$	generated spectral radiation intensity given by Eq. (2)
$L_{\lambda,\mathrm{meas}}$	measured spectral radiation intensity
MRT	multispectral radiation thermometry
n	number of unknown coefficients in emissivity model; index of refraction; number of intersections of surface profile with the mean per unit length of mean line
N	required minimum number of wavelengths in MRT model
Q	radiation heat flux
R	roughness factor
R_a	arithmetic average surface roughness
SRT	spectral radiation thermometry
T	surface temperature
T_λ	spectral radiance temperature

Greek symbols

α_s	absorptivity for smooth surface
β	groove angle
ε_n	normal spectral emissivity
ε_r	effective emissivity for rough surface
ε_s	emissivity for smooth surface
ε_λ	spectral emissivity
ε'_λ	directional emissivity
θ	angle of energy
κ	extinction coefficient
λ	wavelength
ρ_r	reflectance for rough surface
ρ_p	reflectance for polished surface
ρ_λ	spectral reflectance
ρ'_λ	directional reflectance
ρ''_λ	bidirectional reflectance
σ	root-mean-square (rms) surface roughness; standard deviation; mean-square deviation of profile from the mean
ϕ	observation angle
Φ	radiant power flow
χ^2	least-squares error
Ω	solid angle

Subscripts

b	blackbody
gen	generated
i	incident
int	intrinsic
meas	measured
n	normal
r	rough
rad	radiated
s	scattered; smooth
λ	spectral

wavelengths. This results in $n+1$ equations with $n+1$ unknowns: the target surface temperature, T, and n unknown coefficients in the emissivity model. Coates [3] and Doloresco [4] concluded that the exact technique might cause 'over-fitting' and result in large errors when using more than three wavelengths. The second technique, which overcomes the over-fitting problem, is the *least-squares* technique. It employs least squares fitting of the measured radiance values to simultaneously infer emissivity and temperature values. The number of unknown coefficients, n, in the emissivity model must be at least two fewer than the number of spectral radiance values. In other words, spectral intensity must be measured at a minimum of $(n+2)$ wavelengths. The least-squares technique is commonly used in MRT and has been examined by many researchers. The present study is based on this technique.

Using the least-squares technique, the surface temperature and the unknown emissivity coefficients are determined by minimizing the magnitude of

$$\chi^2 = \sum_{i=0}^{n} (L_{\lambda,\mathrm{meas,i}} - L_{\lambda,\mathrm{gen,i}})^2, \tag{1}$$

where $L_{\lambda,\mathrm{meas,i}}$ and $L_{\lambda,\mathrm{gen,i}}$ are the measured and generated values of spectral intensity, respectively. Neglecting the intensity of irradiation from the surroundings that is reflected by the target surface, and applying Planck's blackbody distribution, the generated spectral intensity can be simplified as

$$L_{\lambda,\mathrm{gen}}(\lambda,T) \cong \varepsilon_\lambda(\lambda) L_{\lambda,\mathrm{b}}(\lambda,T) = \varepsilon_\lambda(\lambda)\frac{c_1}{\lambda^5(e^{c_2/\lambda T}-1)}. \tag{2}$$

Previous studies prove surface roughness has a profound influence on spectral emissivity [5–7]. While these effects are widely documented, the relationship between emissivity and surface topography remains quite illusive. In recent studies, the authors of the present study examined eighteen mathematical and analytical emissivity functions in pursuit of better accuracy in determining the temperature of aluminum alloy surfaces [5–7]. Two relatively simple models were deemed most suitable at capturing the emissivity trends.

The main objective of the present study is to develop a more accurate emissivity model that can tackle the complex and diverse operating environment of aluminum processing plants. Such a model should possess sufficient sensitivity in capturing the complex variations of emissivity with wavelength, temperature, alloy and surface roughness. Since the two afore-mentioned models provide adequate compensation for wavelength, temperature and alloy, this study concerns mostly the effects of surface roughness. In particular, a method is sought for incorporating surface roughness parameters in the emissivity model. The next section will explore previous theoretical premises for the relationship between emissivity and surface roughness.

2. Categorization of emissivity principles based on surface roughness

Two broad categories of surfaces can be identified: optically smooth (ideal) and rough (real). Rough surfaces can be further divided into spectral regions based on *optical roughness*, which is represented by the ratio of root-mean-square (rms) surface roughness, σ, to wavelength, λ. The *Specular Region* corresponds to $0 < \sigma/\lambda < 0.2$ and the *Geometric Region* $\sigma/\lambda > 1$. A third *Intermediate Region* can also be identified that corresponds to $0.2 < \sigma/\lambda < 1$. Fig. 1 summarizes theoretical emissivity principles based on surface topography.

2.1. Optically smooth surfaces

For optically smooth surfaces, spectral emissivity is determined by combining Fresnel's equation and Kirchhoff's law yielding

$$\varepsilon_\lambda = \frac{4n^2}{(n+1)^2 + \kappa^2}, \tag{3}$$

where n is the index of refraction and κ the extinction coefficient. The values of these optical constants vary with wavelength, temperature and material composition. These constants are measured experimentally or estimated using electromagnetic or Drude free electron theory [8,9]. Fig. 1(a) compares spectral emissivity values using three different methods: (1) reflectance calculated from measured n and κ values and Kirchhoff's law, (2) experimental reflectance data and Kirchhoff's law, and (3) Drude free electron theory and Fresnel's equation. Both calculated and measured values show a general trend of decreasing emissivity with increasing wavelength in the infrared range for most metallic surfaces. The free electron theory is only limited to ideal optically smooth surfaces and does not capture the trends of the first two methods.

2.2. Rough surfaces

2.2.1. Specular region

In the specular region ($0 < \sigma/\lambda < 0.2$), surface roughness is small compared to the wavelength. Most theoretical models of this region assume the reflection of incident radiation is specular, i.e., the angle of reflection is equal to the angle of incidence, and use the diffraction theory to predict the effects of surface roughness on emissivity [9–11]. For a Gaussian distribution of surface heights, the relationship between reflected radiation and optical roughness has been

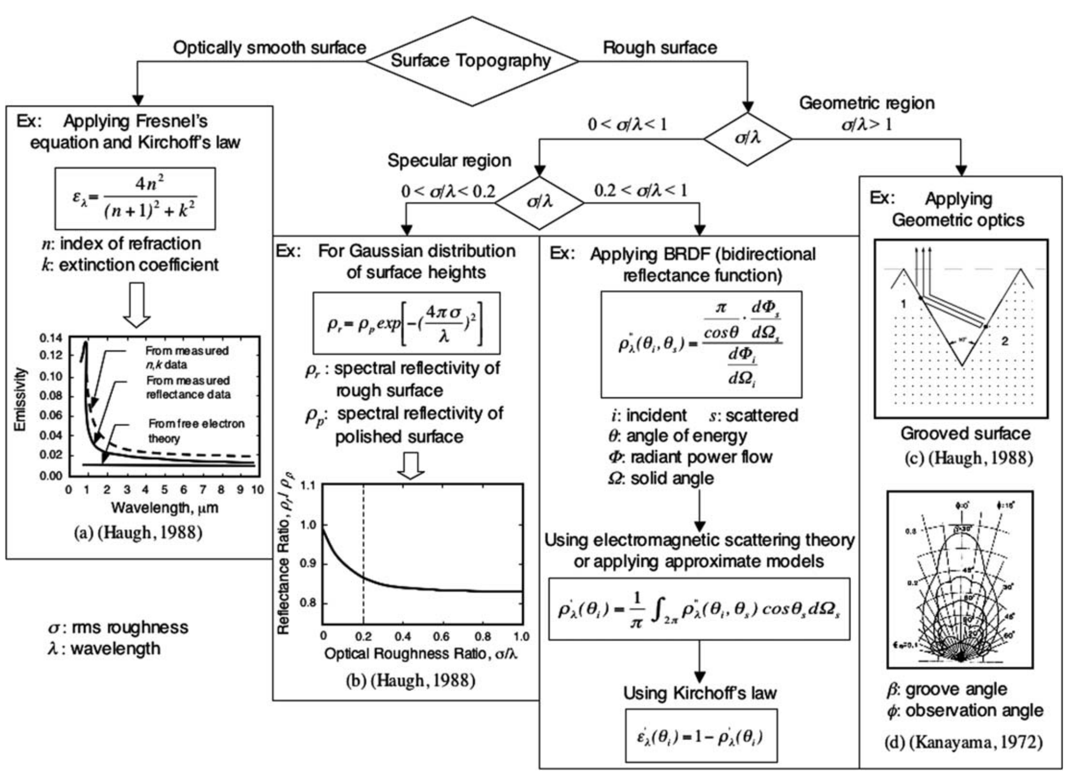

Fig. 1. Classification of emissivity models based on surface roughness.

shown both theoretically [12,13] and experimentally [14,15] to follow an exponential decay function of σ/λ.

$$\rho_r = \rho_p \exp\left[-\left(\frac{4\pi\sigma}{\lambda}\right)^2\right], \tag{4}$$

where ρ_r and ρ_p are the reflectances for a rough surface and a polished surface, respectively. Eq. (4) shows surface roughness can be estimated from the measured reflectance ratio. Fig. 1(b) shows a curve fit of experimental results for the ratio of normal-hemispherical reflectance for a real surface to that for a polished surface versus optical roughness for aluminum-coated ground glass [16]. Since the normal-hemispherical reflectance is equal to $1 - \varepsilon_n$, where ε_n is the normal emissivity, Fig. 1(b) shows a significant decrease in hemispherical reflectance (i.e., increase in emissivity) with optical roughness for $0 < \sigma/\lambda < 0.2$ and a far weaker sensitivity as σ/λ approaches unity.

2.2.2. Intermediate region

When $0.2 < \sigma/\lambda < 1$, the bidirectional reflectance function (BDRF), $\rho''_\lambda(\theta_i, \theta_s)$, is used to quantify the angular reflected radiation [17]. As indicated in Fig. 1, this function is given in terms of the incident and scattered components of angle of energy θ, radiant power flow Φ, and solid angle Ω. Either electromagnetic scattering theory or approximate models are used to estimate the incident and scattered radiant power flow. The directional reflectance, $\rho'_\lambda(\theta_i)$, can be determined by integrating BDRF over the respective hemisphere for a given angle of incidence as indicated in Fig. 1. Using Kirchhoff's law and energy conservation, the directional emissivity can be determined from

$$\varepsilon'_\lambda(\theta_i) = 1 - \rho'_\lambda(\theta_i). \tag{5}$$

A rigorous numerical solution is required to predict the emissivity-roughness relationship for $0.2 < \sigma/\lambda < 1$.

Based on the Extinction and Green's theorems, the electromagnetic scattering theory is an exact approach to quantifying BDRF or other directional features of surface radiative properties [18]. Other approaches involve the use of approximate models to estimate the incident and scattered radiant power flow of BDRF. In the *specular model* (*Fresnel approximation*), energy is assumed to be reflected in the solid angle region around the specular angle, and the fraction of the reflected energy is predicted by Fresnel relations applied to an optically smooth surface [19]. In the *diffuse model* (*Lambertian approximation*), the energy is assumed to be distributed equally in all directions and the bi-directional reflectance is calculated by the cosine law [20]. Because the Fresnel and Lambertian approximations fail to account for surface parameters or incident wavelength effects, *Kirchhoff's approximation* provides reflection distributions between the specular and diffuse reflection models [19–21]. It assumes that the reflected magnetic and electric fields at each point on the surface are equal to the field existing along a plane tangent to the surface at the same point. The *geometric optics approximation* (also called "ray tracing") tracks the energy throughout its interaction with the surface until it leaves the surface [20–22]. Therefore, it includes multiple scatters from various surface elements. The *statistical model* uses geometric optics approximations to predict surface wave scattering, but employs statistical concepts instead of the bundle tracing employed in the geometric optics approximation. The primary elements of statistical models are incoming and outgoing shadowing functions [23]. The incoming shadowing function is defined as the probability that a surface point does not exist in a shadowed region for a given incident angle. This probability is equal to the outgoing shadowing function, which is defined as the probability that an energy bundle reflected at a specified angle will not re-strike the surface.

After examining the aforementioned models, Buckius and co-workers [18–23] concluded that increased roughness increases directional emissivity, and these models yield normal emissivity values that are different for mathematically described surfaces with the same roughness and slope. This proves that slope and roughness are not the only parameters governing the influence of surface topography on emissivity. In other words, additional topographical parameters must be taken into consideration in modeling the intermediate region.

2.2.3. Geometric region

In the geometric region ($\sigma/\lambda > 1$), emissivity is highly sensitive to the detailed surface geometry. Diffraction effects are ignored here because the effects of roughness on emissivity are quite large compared to those of wavelength. Geometric optics are used to predict emissivity once the detailed surface topography is determined. Surfaces with repeatable grooved finish, such as V-shaped grooves [1,24–27], circular grooves [27], and pyramidal grooves [28–30], are commonly used to model the emissivity enhancement. Fig. 1(c) shows inter-reflections caused by a 60° V-groove, which were shown to enhance normal emissivity by a factor of 3.3 [10]. Fig. 1(d) shows appreciable variations of emissivity with observation angle (ϕ) and groove angle (β) for an aluminum surface with a smooth surface normal emissivity of $\varepsilon_n = 0.04$ [26]. For example, a groove angle of 30° produces a seven fold increase in normal emissivity ($\phi = 0$) compared to a smooth surface. For small groove angles, emissivity decreases sharply with increasing observation angle. Therefore, the slope of the grooved surface plays an important role in emissivity enhancement in the geometric region.

The above categorization of surface finishes provides valuable insight into the theoretical emissivity principles and knowledge amassed concerning the relationship between emissivity and surface roughness. Optical roughness ratio is a key parameter commonly used to categorize the influence of surface roughness. Different theories have been proposed to describe the relationship between emissivity and surface roughness for idealized surfaces. Overall, emissivity is dependent on surface roughness for $\sigma/\lambda < 1$, and on surface slope for $\sigma/\lambda > 1$.

Despite these prior efforts, the effects of surface roughness on emissivity remain illusive, and existing emissivity models are inadaptable to practical emissivity measurements, especially in the aluminum industry. This highlights the need for a universal emissivity model that can adequately account for surface topography, and which can be widely adopted throughout the aluminum industry.

3. Experimental methods

An experimental apparatus was configured and fabricated to facilitate accurate emissivity measurements for aluminum alloy samples with different surface topographies and at different temperatures. This apparatus included a spectrometer, a sample heating assembly, and a data acquisition system.

A fast infrared array spectrometer (FIAS) Model ES100 made by Spectraline Inc. was used to simultaneously measure 160 discrete spectral radiation intensity values over a wavelength range of 1.8–4.9 μm. The spectrometer was optically aligned in front of the test sample with the aid of a HeNe laser. Radiation intensity from the target was collected and dispersed over a staggered 160 element linear array PbSe detector. The spectrometer software converted the voltages and pixel numbers from the linear array into wavelengths and intensities.

As shown in Fig. 2, the aluminum sample was mounted along the exterior of a heating assembly consisting of a large aluminum heating block fitted with four cartridge heaters. The block was wrapped in a blanket of ceramic fiber insulation and mounted on a two-dimensional translation stage. Power input to the cartridge heaters was manipulated by a variable voltage transformer.

As shown in Fig. 3, the test samples had a front surface area of $15 \times 15\ \mathrm{mm}^2$. The sample temperature was measured by a thermocouple situated 1 mm behind the surface. Due to the high conductivity of the aluminum samples, the temperature gradient between the thermocouple and the sample's surface was negligible.

The test samples were fabricated from four aluminum alloys: Al-1100, Al-2024, Al-7075, and Al-7150, which span a broad range of domestic and aerospace applications.

To investigate the effects of surface roughness, the samples were treated with four different surface finishes: smooth, roughened with a cloth containing 6 μm diamond compound, roughened with 14 μm grit paper, and extruded. The smooth finish was achieved by a series of five polishing wheels with increasingly finer grit and particle size (320 grit SiC, 400 grit SiC, 600 grit SiC, diamond compound, Gamma alumina). This process created a flat mirror-like polished surface. The 6 μm and 14 μm samples were first treated in the same manner as the smooth before applying the respective final finish. The extruded samples were supplied directly from an Alcoa extrusion plant and cut to the desired size.

The tested samples were cleaned in succession with acetone and methanol to rid the surface of oils, grease, or dirt. The samples were handled with great care, and wrapped in fine tissue to protect them from any contact with roughening agents following the surface preparation.

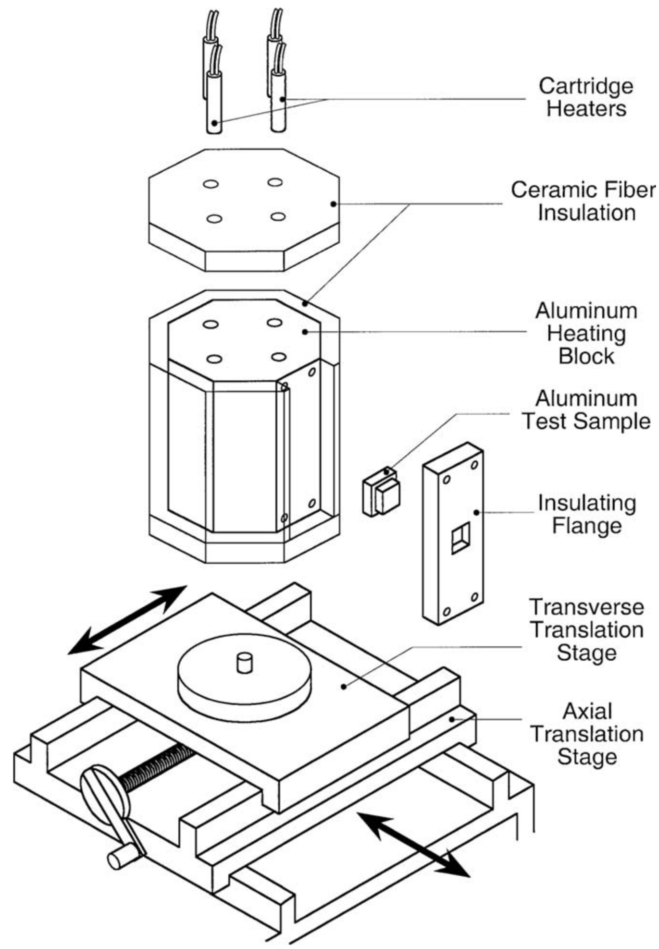

Fig. 2. Construction of sample heating assembly.

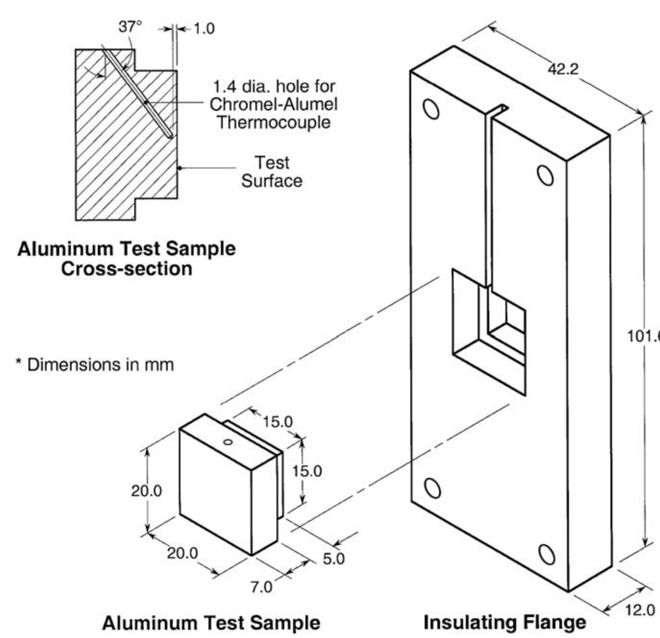

Fig. 3. Construction of aluminum test sample and insulating flange.

The experiments were initiated by preheating the large aluminum block to a temperature slightly above the desired value. Next, a Chromel–Alumel (Type K) thermocouple was inserted into the sample's thermocouple hole, which was pre-packed with high thermal conductivity boron nitride powder in order to ensure good thermal contact between the thermocouple bead and the sample. The sample was inserted in an insulating flange (see Fig. 3) and mounted against the preheated aluminum block. The desired sample temperature was achieved by manipulating the power input to the cartridge heaters. Once the sample temperature reached steady state, both the intensity and temperature data were recorded by the spectrometer. Concurrently, the sample temperature was measured by the thermocouple with the aid of a digit thermometer.

4. Correlation of emissivity with surface roughness parameters

Using geometric optics, Agababov [31] developed a method to determine the emissivity of gray-diffuse rough surfaces having thermal and optical homogeneity. As illustrated in Fig. 4, he modeled local surface roughness as a depression of area A_r and examined all radiation leaving the equivalent smooth surface area A_s, taking into account the effects of reflection from the actual surface A_r. A view factor $F_{r,r}$ is defined as the fraction of the radiation leaving surface A_r that is intercepted by the same surface. Therefore, of the total energy $Q_{int,r}$ radiated from A_r, only the portion $Q_{int,r}(1-F_{r,r})$ will leave through A_s; the balance, $Q_{int,r}F_{r,r}$, will fall back to A_r. A portion of the returned energy, $Q_{int,r}F_{r,r}\alpha_s$, is absorbed by the surface, where α_s is the surface absorptivity, while the other portion, $Q_{int,r}F_{r,r}(1-\alpha_s)$, is reflected by A_r. In the same manner, part of the reflected radiation, $Q_{int,r}F_{r,r}(1-\alpha_s)(1-F_{r,r})$, will leave through A_s, while the balance, $Q_{int,r}F_{r,r}^2(1-\alpha_s)$, will again fall back to A_r. Continuing this absorption/reflection pattern, the total radiation leaving the rough surface through A_s can be expressed as

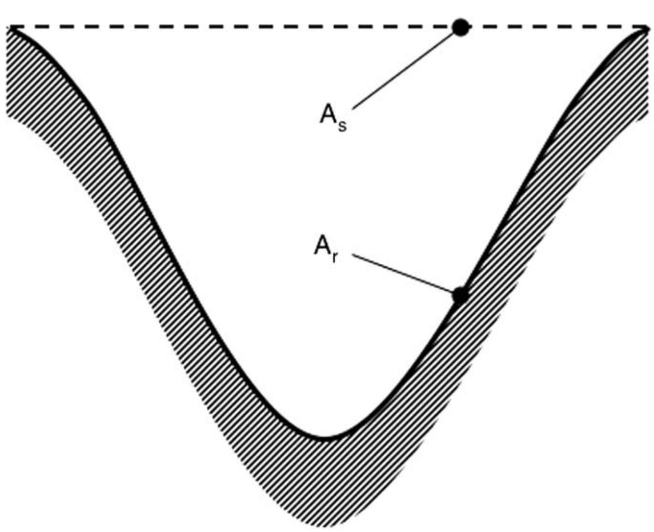

Fig. 4. Idealized representation of roughness feature.

$$Q_{rad,r} = Q_{int,r}(1-F_{r,r})[1+F_{r,r}(1-\alpha_s)+F_{r,r}^2(1-\alpha_s)^2+\cdots]. \tag{6}$$

The expression in the square brackets represents a decreasing infinite geometric series, which reduces Eq. (6) to

$$Q_{rad,r} = Q_{int,r}(1-F_{r,r})\frac{1}{1-(1-\alpha_s)F_{r,r}}. \tag{7}$$

The components of radiation are defined as

$$Q_{int,r} = \varepsilon_s E_b A_r \tag{8a}$$

and

$$Q_{rad,r} = \varepsilon_r E_b A_s. \tag{8b}$$

Eq. (8a) represents the intrinsic radiation of surface A_r with the emissivity of the smooth surface ε_s and the latter the radiation passing through surface A_s. Substituting Eqs. (8a) and (8b) into Eq. (7) yields

$$\varepsilon_r = \varepsilon_s\frac{A_r}{A_s}(1-F_{r,r})\frac{1}{1-(1-\alpha_s)F_{r,r}}. \tag{9}$$

For the geometry shown in Fig. 4, the view factor is given by

$$F_{r,r} = 1-\frac{A_s}{A_r}, \tag{10}$$

and the roughness factor by

$$R = \frac{A_s}{A_r}. \tag{11}$$

Therefore, for a gray body ($\varepsilon = \alpha$), Eq. (9) can be expressed as

$$\varepsilon_r = \left[1+\left(\frac{1}{\varepsilon_s}-1\right)R\right]^{-1}, \tag{12}$$

where ε_r and ε_s are the effective emissivities of the rough surface and smooth surface, respectively. This relationship is also valid for non-gray bodies if the series in the square brackets in Eq. (6) converges sufficiently rapidly. Eq. (12) can also be used to relate the emissivities ε_i and ε_k for surfaces with different roughness factors, R_i and R_k, respectively, but the same material (i.e. equal ε_s),

$$\varepsilon_i = \left[1+\left(\frac{1}{\varepsilon_k}-1\right)\frac{R_i}{R_k}\right]^{-1}. \tag{13}$$

Agababov [32,33] experimentally demonstrated how the roughness factor can be implemented in determining the radiative properties. If the roughness is regularly distributed, the roughness factor can be calculated in a relatively straightforward manner [31]. However, if the roughness distribution is random, the roughness factor can be calculated from a profilogram of the surface [34,35]. Specifically, for an isotropic rough surface having small surface inclinations,

$$R = (1+\pi^2 n^2 \sigma^2)^{-1}, \tag{14}$$

where n is the number of intersections of the surface profile with the mean per unit length of the mean line, and σ the mean-square deviation of the profile from the mean. For most rough surfaces, σ can be expressed in terms of the mean arithmetic deviation, R_a, of the profile according to the relation $\sigma \approx 1.25R_a$, where R_a is measured by a profilometer or other surface measurement instrument. Therefore Eq. (14) can be simplified as

$$R = (1 + 1.25^2\pi^2 n^2 R_a^2)^{-1}. \quad (15)$$

Eqs. (12) and (15) show how the emissivity of a rough surface can be related to the surface roughness parameters. This method also provides a fundamental basis for the development of a new more comprehensive emissivity model that can accurately compensate for emissivity variations with surface roughness. Eq. (13) further shows how the emissivity of a rough surface can be determined from a known emissivity value of another rough surface of the same material, provided the surface roughness parameters (n and R_a) of both surfaces are known.

Since this model is based on geometric optics, it may also be incorporated in spectral variations of emissivity. This was accomplished by using the experimental data obtained in the present study for AL7075. The polished surface was used as a reference for the other rougher surfaces. As shown in Table 1, the surface parameters were measured for the four different surface finishes. An Alpha-Step IQ surface profiler, made by KLA-Tencor, and a MicroXam microscope, made by Phase Shift Technology, were used to measure R_a and σ. The number, n, of intersections of the surface profile with the mean per unit length of the mean line was manually calculated through the surface profilogram as illustrated in Fig. 5, and R was calculated using Eq. (14) or (15). Eq. (13) was finally used to predict emissivity values for a given rough surface (i) using the measured emissivity of the smooth surface (k) as a reference.

Figs. 6–8 compare the measured emissivity values at 600 and 700 K for the 6 μm, 14 μm, and extruded surfaces, respectively, with predictions based on Eq. (13). Overall, good agreement is achieved for all three surfaces and the agreement appears to improve with increasing temperature.

These findings prove the emissivity model proposed by Agababov [31–35] provides a simple yet effective means for both modeling the surface roughness parameters and relating emissivity to these parameters. This represents an important step toward developing a comprehensive emissivity model that could account for all the complex parametric trends of aluminum alloys.

Table 1
Surface parameters of AL7075 samples

Surface	R_a (μm)	σ (μm)	n (1/μm)	R
Smooth	0.076	0.111	0.193	0.9967
Roughened with 6 μm diamond compound	0.146	0.209	0.176	0.9899
Roughened with 14 μm grit paper	0.344	0.444	0.098	0.9828
Extruded	4.55	5.16	0.0133	0.9465

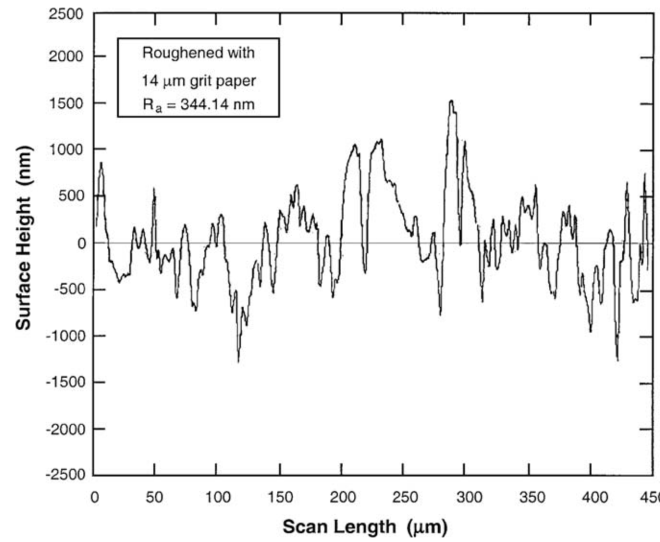

Fig. 5. Profilogram of AL 7075 sample roughened with 14 μm grit paper.

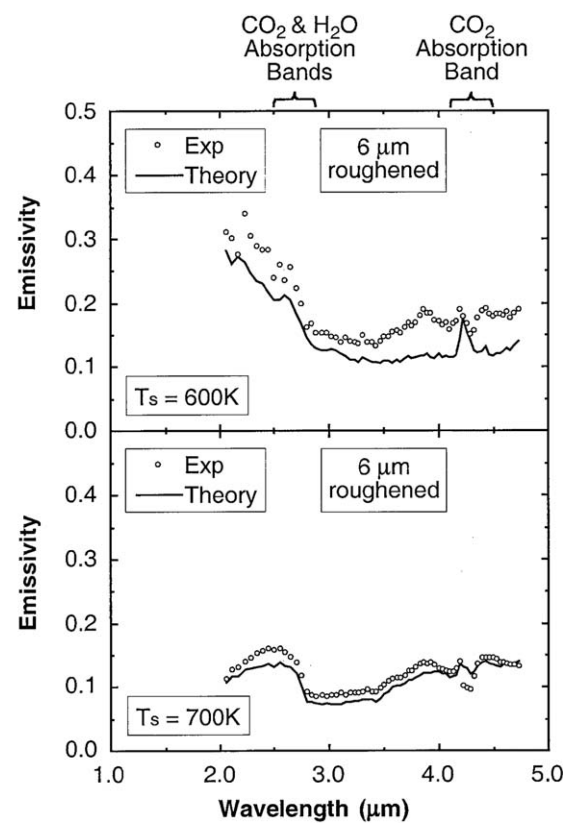

Fig. 6. Comparison of experimental and theoretical spectral emissivity values for AL 7075 samples roughened with 6 μm diamond compound at 600 and 700 K.

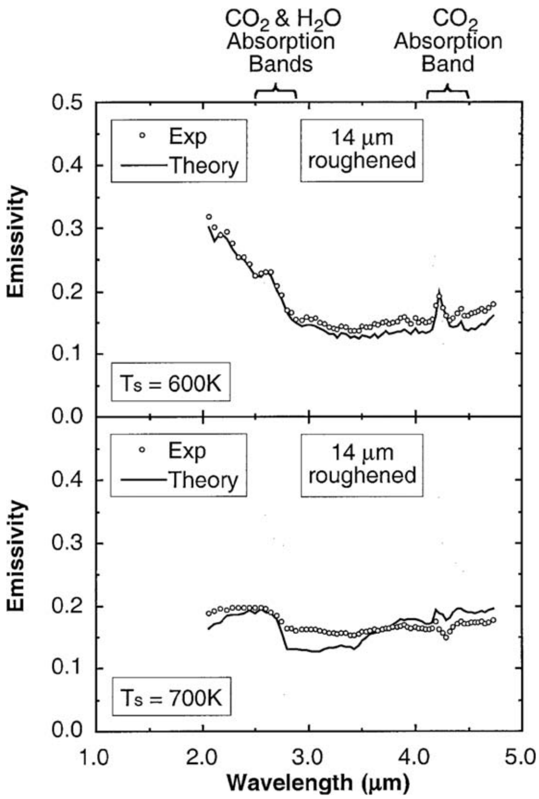

Fig. 7. Comparison of experimental and theoretical spectral emissivity values for AL 7075 samples roughened with 14 μm grit paper at 600 and 700 K.

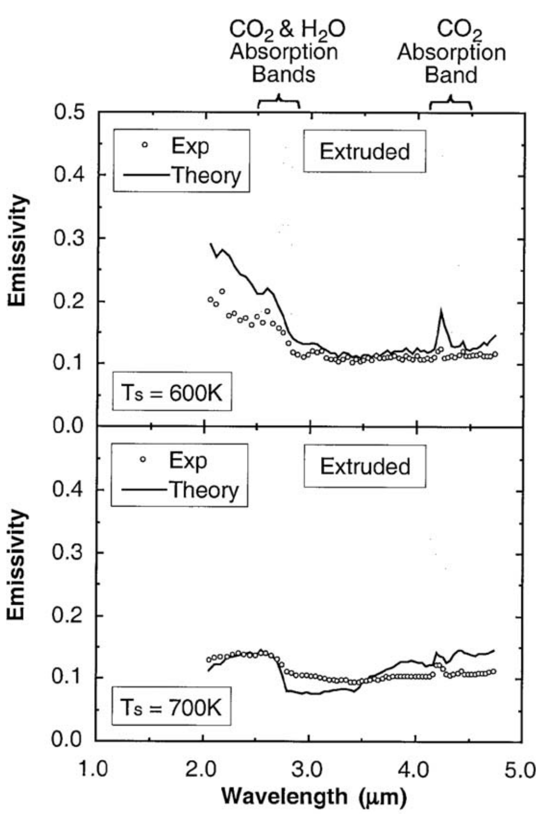

Fig. 8. Comparison of experimental and theoretical spectral emissivity values for extruded AL 7075 samples at 600 and 700 K.

5. Application of MRT emissivity models

Figs. 9 and 10 compare, for different temperatures and alloys, respectively, the present experimental reflectance data with Birkebak and Eckert's [16] data for aluminum-coated glass corresponding to the specular region. Higher values were measured in the present study, yet the overall trends are similar for both studies. The present range corresponds to the specular range for rough surfaces, and the corresponding trend is one of decreasing reflectance (i.e., increasing emissivity) with increasing optical ratio.

Recently, the authors of the present study presented a comprehensive experimental assessment of emissivity trends for smooth and roughened aluminum alloy surfaces [5–7]. Their measurements were also used to assess eighteen MRT emissivity models. Two relatively simple MRT emissivity models, an exponential function of $1/T_\lambda$ (where T_λ is the equivalent blackbody temperature of the measured spectral emissivity) and an exponential of a linear first order function of $\sqrt{\lambda}$, provided the best overall compensation for different alloys, temperatures, and surface roughness.

In the present study, these models were used to predict the effects of alloy, temperature and wavelength. As shown

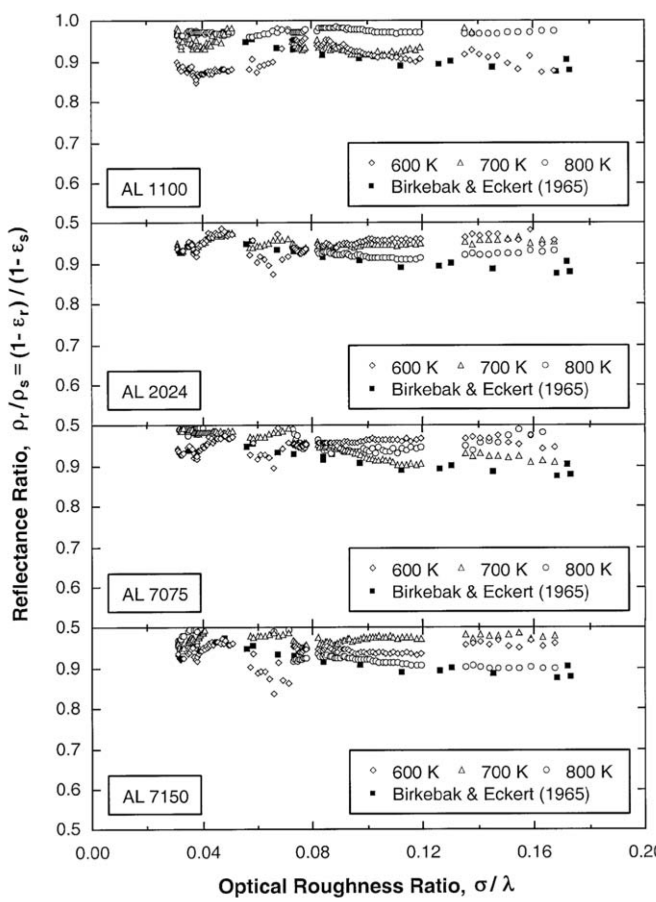

Fig. 9. Ratio of normal hemispherical reflectance of rough surface to that for smooth surface as a function of optical roughness ratio at different temperatures.

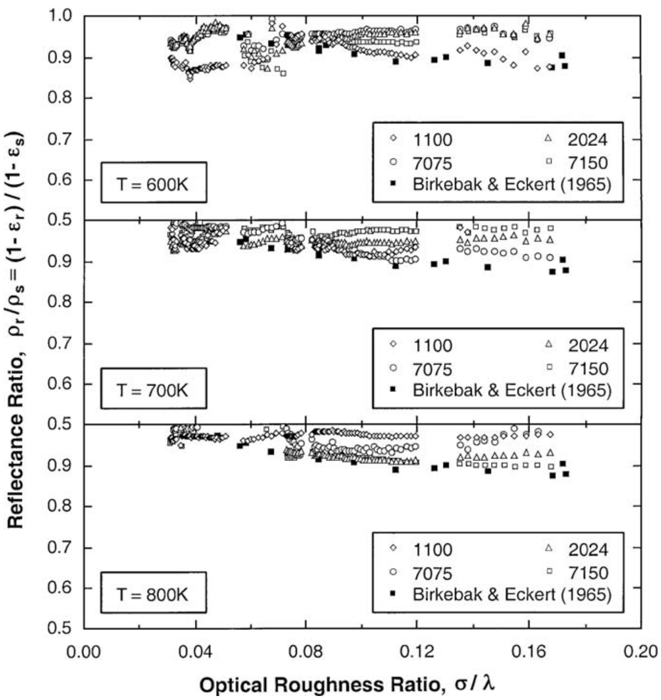

Fig. 10. Ratio of normal hemispherical reflectance of rough surface to that for smooth surface as a function of optical roughness ratio for different alloys.

in Table 2, these models include the two aforementioned best models and two variations of the same models. The four models were tested in two ways, in their basic form and modified with the roughness function proposed by Agababov. When testing a basic model, only data for that surface were used. On the other hand, the modified model was applied by referencing emissivity data for the rough surface (i) to that for the smooth surface (k) using Eq. (13).

For this study, the AL7075 14-μm roughened surface (i) and smooth surface (k) were examined. The respective roughness factors were calculated according to Eq. (15) using the measured values of n and R_a given in Table 1. The least-squares technique and numerical iterations were used to simultaneously determine the surface temperature and values of coefficients in the emissivity model. The primary goal here is to examine whether the new emissivity models that include the surface roughness parameters can more effectively account for the complex variations of emissivity than the basic emissivity models.

Table 3 provides absolute errors in the inferred temperatures for measured surface temperatures at 600 and 700 K for AL 7075 samples roughened with 14-μm grit paper. In order to investigate the effects of number of wavelength in the MRT method, three different numbers of wavelengths, N, $N+1$ and $N+2$, were examined, where N is the required minimum number of wavelengths. Also, three spectral ranges: a short range of 2.05–3.43 μm, a long range of 3.50–4.72 μm, and a combined range of 2.05–4.72 μm, were examined. Data in two bands were excluded from the analysis due to the appreciable error atmospheric absorption and scattering contribute to radiation intensity in these bands. The first band (centered at 2.7 μm) is influenced by H_2O (room humidity) and CO_2 molecules, and

Table 2
Mathematical form of emissivity models examined in this study

Emissivity model	Mathematical function
Agababov	$\varepsilon_i = \left[1 + \left(\frac{1}{\varepsilon_k} - 1\right)\frac{R_i}{R_k}\right]^{-1}, R = (1 + 1.25^2\pi^2 n^2 R_a^2)^{-1}$
base1	$\varepsilon_\lambda = \exp(a_0/T_\lambda)$
mod1	$\varepsilon_{\lambda,i} = \left[1 + \left(\frac{1}{\exp(a_0/T_\lambda)} - 1\right)\frac{R_i}{R_k}\right]^{-1}$
base2	$\varepsilon_\lambda = \exp(a_0\sqrt{\lambda})$
mod2	$\varepsilon_{\lambda,i} = \left[1 + \left(\frac{1}{\exp(a_0\sqrt{\lambda})} - 1\right)\frac{R_i}{R_k}\right]^{-1}$
base3	$\varepsilon_\lambda = \exp(a_0\sqrt{\lambda}/T_\lambda)$
mod3	$\varepsilon_{\lambda,i} = \left[1 + \left(\frac{1}{\exp(a_0\sqrt{\lambda}/T_\lambda)} - 1\right)\frac{R_i}{R_k}\right]^{-1}$
base4	$\varepsilon_\lambda = \exp[\sqrt{\lambda}/(a_0 + a_1 T_\lambda)]$
mod4	$\varepsilon_{\lambda,i} = \left[1 + \left(\frac{1}{\exp[\sqrt{\lambda}/(a_0+a_1 T_\lambda)]} - 1\right)\frac{R_i}{R_k}\right]^{-1}$

T_λ is spectral radiance temperature defined as equivalent blackbody temperature of measured spectral intensity.

Table 3
Absolute error in inferred temperature of AL7075 samples roughened with 14 μm grit paper

Mode 1	N	600 K			700 K		
		Wavelength (μm)			Wavelength (μm)		
		2.05–3.43	3.50–4.72	2.05–4.72	2.05–3.43	3.50–4.72	2.05–4.72
base1	N			27.5	−0.5		−21.9
	$N+1$			27.2	3.0		−22.3
	$N+2$			26.8	4.7		−22.0
mod1	N	49.1		−9.9	−6.7		−20.0
	$N+1$	47.3		−11.1	6.5		−17.8
	$N+2$			−11.9	5.5		−20.5
base2	N	41.9		1.6	−27.5		−47.5
	$N+1$	43.0		−0.4	−24.1		−48.6
	$N+2$	44.8		−0.6	−22.7		−48.3
mod2	N	23.1		−3.2	−34.6		−38.2
	$N+1$	35.4		−5.1	−22.1		−41.3
	$N+2$	34.8		−5.9	−23.4		
base3	N	16.3		−12.7	−42.1		
	$N+1$	16.1		−15.0	−39.8		
	$N+2$	17.2		−15.9	−38.8		
mod3	N	−4.2		12.3	−41.7		
	$N+1$	5.5		15.5	−41.6		47.0
	$N+2$	4.7		8.4	−42.7		45.5
base4	N	39.2		−10.7			−21.1
	$N+1$	42.3		−5.3	−47.1		−15.1
	$N+2$	30.5		−13.4			−23.4
mod4	N	27.5		−10.2	−24.6		−37.4
	$N+1$	27.9		−8.1	−45.7		
	$N+2$	34.4		−8.9			

Missing values correspond to errors.
N is minimum number of wavelengths required in MRT model, which is equal to number of unknown coefficients in model plus two.

the other (centered at 4.3 μm) by CO_2 molecules alone. To simplify the identification of accurate models, only errors below ± 50 K are given in the table. The results of each basic mathematical emissivity model are compared with those for the same model modified with the Agababov expression for surface roughness.

At a first glance, both the basic and modified models appear to provide acceptable results in the same spectral regions. However, the modified models provide better overall emissivity compensation than the original models. Regarding the effects of spectral range, Table 3 shows "acceptable results" are concentrated primarily in the combined spectral range (2.05–4.72 μm) or in the short range (2.05–3.43 μm), but not the long range. Therefore, broadening the wavelength range to encompass all measured wavelengths may not always enhance the predictive capability of an emissivity model. In addition, the minimum number of wavelengths, N, required by the least squares MRT technique generally seems to yield satisfactory results. Therefore, increasing the number of wavelengths (i.e. using $N+1$ or $N+2$) does not improve predictive accuracy. Of the four modified emissivity models, model 4 shows the poorest compensation for emissivity variations at 700 K. In contrast, modified models 1 and 3 are better at compensating for emissivity variations at 700 and 600 K, respectively. Overall, modified model 2 provides the best overall compensation for different temperatures.

In summary, all four modified models are successful at incorporating surface roughness parameters and provide temperature predictions superior to those of the original mathematical models.

6. Conclusions

This study explored the relationship between the emissivity of aluminum alloy surfaces and surface roughness. Different theory governing this relationship were reviewed and categorized. A previous model by Agababov was found to be an effective means for both characterizing surface roughness and incorporating roughness features in emissivity models. Four emissivity models were examined based on their proven accuracy at determining both emissivity and surface temperature using the MRT technique. Those models were tested both in their basic form and modified with the Agababov roughness function for accuracy in inferring surface temperatures of Al 7075 samples. Key findings from the study are as follows:

(1) Overall, good agreement is achieved between measured emissivity values and predictions based on the Agababov roughness function. This agreement appears to improve with increasing temperature. This shows this roughness function is an effective means for representing surface roughness features and accounting for the effects of surface roughness on emissivity.
(2) Temperature predictions of the four emissivity models were examined using both the basic form of these models as well as by modifying them with the Agababov roughness function. Both the basic and modified forms provide acceptable results in the same spectral regions. However, the accuracy of the modified models is superior to those of their basic counterparts. This shows the modified models provide adequate compensation for the effects of wavelength, temperature and surface roughness in MRT models.
(3) Broadening the wavelength range to encompass all measured wavelengths may not always enhance the predictive capability of an emissivity model. In addition, increasing the number of wavelengths in the MRT model does not improve predictive accuracy.
(4) Overall, a simple exponential emissivity function of $\sqrt{\lambda}$, modified with the Agababov roughness function, provides the best overall predictions for different temperatures.

Acknowledgements

The authors gratefully acknowledge the financial support of the Indiana 21st Century Research and Technology Fund, Mr. Gerry Dail of Alcoa for providing the aluminum samples, and Dr. Jongmook Lim of Spectraline for his technical assistance.

References

[1] G.J. Dail, M.G. Fuhrman, D.P. DeWitt, Evaluation and extension of the spectral-ratio radiation thermometry method, in: Proc. 4th Int. Aluminum Extrusion Technology Seminar, Chicago, IL, vol. 2, April, 11–14, 1988, pp. 281–286.
[2] M.A. Pellerin, Multispectral Radiation Thermometry for Industrial Applications, Ph.D. thesis, Purdue University, West Lafayette, IN, 1999.
[3] P.B. Coates, Multi-wavelength pyrometry, Metrologia 17 (1981) 103–109.
[4] B.K. Doloresco, Review of Multispectral Radiation Thermometry and Development of Constrained Minimization Method, M.S. thesis, Purdue University, West Lafayette, IN, 1986.
[5] C. Wen, I. Mudawar, Experimental investigation of emissivity of aluminum alloys and temperature determination using multispectral radiation thermometry (MRT) algorithms, J. Mater. Eng. Perform. 11 (2002) 551–562.
[6] C. Wen, I. Mudawar, Emissivity characteristics of polished aluminum alloy surfaces and assessment of multispectral radiation thermometry (MRT) emissivity models, Int. J. Heat Mass Transfer 48 (2005) 1316–1329.
[7] C. Wen, I. Mudawar, Emissivity characteristics of roughened aluminum alloy surfaces and assessment of multispectral radiation thermometry (MRT) emissivity models, Int. J. Heat Mass Transfer 47 (2004) 3591–3605.
[8] M.F. Modest, Radiative Heat Transfer, McGraw-Hill, New York, NY, 1993.
[9] D.P. DeWitt, J.C. Richmond, Thermal radiative properties of materials, in: D.P. DeWitt, G.D. Nutter (Eds.), Theory and Practice of Radiation Thermometry, John Wiley, New York, NY, 1988.
[10] R. Siegel, J.R. Howell, Thermal Radiation Heat Transfer, McGraw-Hill, New York, NY, 1981.
[11] M.J. Haugh, Radiation thermometry in the aluminum industry, in: D.P. DeWitt, G.D. Nutter (Eds.), Theory and Practice of Radiation Thermometry, John Wiley, New York, NY, 1988.

[12] H. Davis, Reflection of electromagnetic waves from rough surfaces, Proc. Inst. Eng. 101 (1954) 209–213.
[13] J.O. Porteus, Relation between the height distribution of a rough surface and the reflection of normal incidence, J. Opt. Soc. Amer. 53 (1963) 1394–1402.
[14] H.E. Bennett, J.O. Porteus, Relation between surface roughness and specular reflectance at normal incidence, J. Opt. Soc. Am. 51 (1961) 123–129.
[15] H.E. Bennett, Specular reflectance of aluminized ground glass and the height distribution of surface irregularities, J. Opt. Soc. Am. 53 (1963) 1389–1394.
[16] R.C. Birkebak, E.R.G. Eckert, Effect of metal surface on the angular distribution of monochromatic reflected radiation, Trans. ASME 87C (1965) 85–94.
[17] M.Q. Brewster, Thermal Radiative Transfer and Properties, John Wiley, New York, NY, 1992.
[18] R.A. Dimenna, R.O. Buckius, Electromagnetic theory predictions of the directional scattering from triangular surfaces, Trans. ASME 116 (1994) 639–645.
[19] R.A. Dimenna, R.O. Buckius, Quantifying specular approximations for angular scattering from perfectly conducting random rough surfaces, J. Thermophys. Heat Transfer 3 (1994) 393–399.
[20] K. Tang, R.A. Dimenna, R.O. Buckius, The geometric optics approximation for reflection from two-dimensional random rough surfaces, Int. J. Heat Mass Transfer 41 (1997) 2037–2047.
[21] J.A. Ogilvy, Wave scattering from rough surfaces, Reports Progr. Phys. 50 (1987) 1553–1608.
[22] K. Tang, R.A. Dimenna, R.O. Buckius, Regions of validity of the geometric optics approximation for angular scattering from very rough surfaces, Int. J. Heat Mass Transfer 40 (1997) 49–59.
[23] K. Tang, R.A. Dimenna, R.O. Buckius, A statistical model of wave scattering from random rough surfaces, Int. J. Heat Mass Transfer 44 (2001) 4059–4073.
[24] R.B. Zipin, The Directional Spectral Reflectance of Well-Characterized Symmetric V-Grooved Surfaces, Ph.D. Thesis, Purdue University, West Lafayette, IN, 1965.
[25] R.B. Zipin, A preliminary investigation of the bidirectional spectral reflectance of V-grooved surfaces, Appl. Opt. 5 (1966) 1954–1957.
[26] R.G Hering, T.F. Smith, Apparent radiation properties of a rough surface, AIAA Paper no. 69–622, 1969.
[27] K. Kanayama, Apparent directional emittances of V-groove and circular-groove rough surfaces, Heat Transfer – Jpn. Res. 1 (1972) 11–22.
[28] A. Abdulkadir, R.C. Birkebak, Optical surface roughness and slopes measurements with a double beam spectrophotometer, Rev. Sci. Instrum. 45 (1974) 1356–1360.
[29] A. Abdulkadir, R.C. Birkebak, Spectral directional emittance of metal surfaces with pyramidal surface undulation, Proc. 5th Int. Heat Transfer Conf., Tokyo (1974) 21–25.
[30] A. Abdulkadir, R.C. Birkebak, Effects of large pyramidal surface roughness on spectral directional emittance, Warme- und Stoffubertragung 10 (1977) 23–32.
[31] S.G. Agababov, Effect of the roughness of the surface of a solid body on its radiation properties and methods for their experimental determination, Teplofizika Vysokikh Temperature 6 (1968) 78–87.
[32] S.G. Agababov, Effect of secondary roughness on the emissive properties of solid bodies, Teplofizika Vysokikh Temperature 8 (1970) 220–222.
[33] S.G. Agababov, Effect of the roughness factor on radiation properties of solids, Teplofizika Vysokikh Temperature 8 (1970) 770–773.
[34] S.G. Agababov, L.I. Eksler, Influence of the geometric characteristics of the relief of the surface of a solid on its radiation properties, Teplofizika Vysokikh Temperature 9 (1971) 522–526.
[35] S.G. Agababov, Effect of roughness factor on the radiation properties of a solid body with random roughness, Teplofizika Vysokikh Temperature 13 (1975) 314–317.